

Original Article

ABCG2-overexpressing S1-M1-80 cell xenografts in nude mice keep original biochemistry and cell biological properties

Fang Wang, Yong-Ju Liang, Xing-Ping Wu, Xiao-Dong Su and Li-Wu Fu

Abstract

S1-M1-80 cells, derived from human colon carcinoma S1 cells, are mitoxantrone-selected ABCG2-overexpressing cells and are widely used in *in vitro* studies of multidrug resistance (MDR). In this study, S1-M1-80 cell xenografts were established to investigate whether the MDR phenotype and cell biological properties were maintained *in vivo*. Our results showed that the proliferation, cell cycle, and ABCG2 expression level in S1-M1-80 cells were similar to those in cells isolated from S1-M1-80 cell xenografts (named xS1-M1-80 cells). Consistently, xS1-M1-80 cells exhibited high levels of resistance to ABCG2 substrates such as mitoxantrone and topotecan, but remained sensitive to the non-ABCG2 substrate cisplatin. Furthermore, the specific ABCG2 inhibitor Ko143 potently sensitized xS1-M1-80 cells to mitoxantrone and topotecan. These results suggest that S1-M1-80 cell xenografts in nude mice retain their original cytological characteristics at 9 weeks. Thus, this model could serve as a good system for further investigation of ABCG2-mediated MDR.

Key words Multidrug resistance, xenograft, S1-M1-80, ABCG2, nude mice

Multidrug resistance (MDR), a well defined phenomenon in which cancer cells become resistant to a variety of anticancer drugs with different structures and mechanisms of action, is a major obstacle towards curative cancer chemotherapy. Among the diverse mechanisms responsible for MDR phenotype, a common cause is the overexpression of ATP-binding cassette (ABC) transporters such as ABC subfamily B member 1 (ABCB1; also called P-glycoprotein, P-gp), ABC subfamily C members (ABCCs; also called MDR-associated proteins, MRPs), and ABC subfamily G member 2 (ABCG2; also called breast cancer resistance protein, BCRP)^[1-3]. ABCG2 is a 655 amino acid glycoprotein that contains 1 ATP-binding domain and 6 transmembrane domains^[4]. It is physiologically expressed in a variety of tissues, most abundantly in the liver and intestinal epithelia, placenta, blood-brain barrier, and

various stem cells^[5-7]. Unlike P-gp and MRP1, which are arranged in 2 repeated halves, ABCG2 is a half-transporter consisting of only 1 nucleotide-binding domain followed by 1 membrane-spanning domain. The half-transporter can transport a diverse array of substrates, including anticancer agents such as mitoxantrone, camptothecin and its analogs (e.g., diflomotecan, a synthetic derivative of camptothecin), and flavopiridol, a promising drug in clinical development^[8-10].

Numerous studies have shown that elevated ABCG2 expression in clinical specimens of both solid and hematologic cancers, including esophageal squamous cell carcinoma^[11] and acute myeloid leukemia^[12-14], is associated with poor prognosis. In a retrospective study of non-small cell lung cancer, chemotherapy response rate in patients was correlated with ABCG2 expression but not with the expression of ABCB1, ABCC1, or ABCC3, suggesting that specific inhibition of ABCG2 function may help to overcome drug resistance in these patients^[15]. These findings have important potential implications for the strategy of targeting ABCG2 as a part of cancer therapy.

As an energy-dependent drug efflux pump, ABCG2 extrudes a variety of xenobiotics and drugs from cells, thereby mediating resistance to these agents and

Authors' Affiliation: State Key Laboratory of Oncology in South China, Sun Yat-sen University Cancer Center, Guangzhou, Guangdong 510060, P. R. China

Corresponding Author: Li-Wu Fu, State Key Laboratory of Oncology in South China, Sun Yat-sen University Cancer Center, Guangzhou, Guangdong 510060, China. Tel: +86-20-87343163, Fax: +86-20-87343392, Email: fulw@mail.sysu.edu.cn.

doi: 10.5732/cjc.011.10310

affecting their pharmacologic behavior^[16]. It is worth noting that mutations of amino acid 482 in ABCG2 facilitate substrate selection. ABCG2 variants containing either R482G or R482T conferred increased mitoxantrone resistance to transfected cells. Moreover, these variants introduced anthracyclin (doxorubicin) resistance and rhodamine-123 extrusion capacity, which was not observed for the wild-type protein. In contrast, the R482G and R482T mutants were not able to extrude methotrexate, which is a transport substrate of wild-type ABCG2^[17].

Many *in vitro* experimental models have been developed to better understand the mechanisms of drug resistance. The functionally relevant *in vivo* model has been an important method to study drug resistance and evaluate new effective therapies. S1-M1-80 cells derived from human colon carcinoma S1 cells are mitoxantrone-selected ABCG2-overexpressing cells carrying the R482G variant and have been widely used for MDR research *in vitro*. To determine whether S1-M1-80 cells in xenografts maintained the MDR phenotype and the biological properties observed *in vitro*, we established the S1-M1-80 cell xenograft model in nude mice and investigated the biological properties of the drug-resistant xenograft cells.

Materials and Methods

Drugs and antibodies

Doxorubicin, mitoxantrone, topotecan, cisplatin, collagenase, 3-(4, 5-Dimethylthiazol-2-yl)-2, 5-diphenyl-tetrazolium bromide (MTT), rhodamine 123, and other chemicals were purchased from Sigma Chemical Co (St. Louis, MO, USA). The P-gp, MRP1, and ABCG2 monoclonal antibodies were purchased from Santa Cruz Biotechnology (Delaware, USA). Ko143, a selective pharmacological inhibitor of ABCG2, was kindly provided by Dr. Kenneth Kin Wah To (The Chinese University of Hong Kong).

Cell lines and cell culture

The following cell lines were cultured in DMEM or RPMI-1640 supplemented with 10% fetal bovine serum, 100 units/mL penicillin, and 100 mg/mL streptomycin at 37°C in the presence of 5% CO₂: the human oral epidermoid carcinoma cell line KB and its vincristine-selected derivative ABCB1-overexpressing cell line KBv200^[18], which were a gift from Dr. Xu-Yi Liu (Cancer Hospital of Beijing, Beijing, China); the human epidermoid carcinoma cell line KB-3-1 and its doxorubicin-selected derivative ABCC1-overexpressing cell line CA120^[19], which were kindly provided by Dr.

Shin-ichi Akiyama (Kagoshima University, Kagoshima, Japan); and the colon carcinoma cell line S1 and its mitoxantrone-selected derivative ABCG2-overexpressing cell line S1-M1-80^[20], which were kindly provided by Dr. S.E. Bates (National Cancer Institute, NIH, Bethesda, MD). KB and KBv200 cells were used as negative and positive controls, respectively, for the detection of ABCB1 expression. KB-3-1 and CA120 cells were used as negative and positive controls, respectively, for the detection of ABCC1 expression.

Animals and establishment of the drug resistance model

BALB/c nude mice of both sexes, 6-8 weeks old, were purchased from Shanghai Slike Experimental Animals Co. (animal experimental license No. SCXKhu2007-0005, Shanghai, China) and raised under specific pathogen-free conditions. S1-M1-80 cells were suspended at 1×10^6 cells/mL in phosphate-buffered saline (PBS), and 200 μ L of this suspension (2×10^7 cells) was subcutaneously injected into the right flank of athymic nude mice. Tumors were measured using electronic calipers every week for 63 days. Tumor size was calculated according to the following formula: tumor volume = $\pi/6 \times L \times W^2$, with L and W representing the longest and the shortest tumor diameters, respectively.

Isolation of xS1-M1-80 cells

Fresh xenografts of S1-M1-80 cells separated from nude mice were mechanically disaggregated with sterile crossed scalpels to obtain pieces of about 1 mm³. After cutting, the tissue was resuspended in 5 volumes of digestion solution [collagenase sigma type 1 (40 units/mL of growth medium)] and incubated at 37°C for 3 h. Single xS1-M1-80 cell suspension solution was obtained after the solution was filtered through a 200-mesh sieve.

Cytotoxicity assay

Drug cytotoxicity was assessed *in vitro* using the MTT assay as previously described^[21]. S1-M1-80 and xS1-M1-80 cells were seeded in 96-well plates in growth medium (200 μ L/well) containing various concentrations of drugs for 68 h at 37°C in the presence or absence of the specific inhibitor Ko143. Then, 20 μ L of MTT (5 mg/mL) was added to each well for another 4-hour incubation. The resulting purple precipitate in each well was dissolved in 100 μ L DMSO, and the absorbance at 540 nm (A_{540}) was measured, with background subtraction at 655 nm, using the Model 550 Microplate Reader (BIO-RAD, Hercules, CA, USA). The concentrations required to inhibit cell growth by 50%

(IC₅₀) were calculated from survival curves using the Bliss method^[22]. The degree of resistance was calculated by dividing the IC₅₀ for the MDR cells by that for the parental sensitive cells. The fold-reversal factor of MDR was calculated by dividing the IC₅₀ for cells with the anticancer drug in the absence of Ko143 by that obtained in the presence of Ko143. All experiments were performed in triplicate.

Cell proliferation assay and cell cycle

Cells at exponential growth phase were seeded in 96-well plates (2000 cells/well) in growth medium. Then, MTT (5 mg/mL) was added to the wells (20 µL/well) every 24 h for 5 consecutive days. The A₆₄₀ was detected, with background subtraction at 655 nm. Cell proliferation rate was calculated as follows: $[(A_{\text{exp}} - A_{\text{blank}}) - (A_0 - A_{\text{blank}})] / (A_0 - A_{\text{blank}}) \times 100\%$, where A₀ referred to the absorbance value at the onset of experiment and A_{exp} referred to the absorbance values of the experimental cells. The cell proliferation curves were plotted^[23].

Cell ploidy was used to assess cell cycle status. Exponentially growing cells were harvested, fixed with cold 70% ethanol overnight, washed twice with 1× PBS, and stained with propidium iodide (100 µg/mL) containing RNase A (100 µg/mL) for 30 min at 37°C in the dark. Cell cycle was detected using a flow cytometer (Beckman-Coulter, Miami, FL). The percentages of the cell population at different phases were calculated from histograms using the CellQuest software (BD Sciences, San Jose, CA, USA).

Western blot analysis

Total cell lysate was prepared from 1 × 10⁶ cells by adding 100 µL of lysis buffer (1× PBS, 1% NP40, 0.5% sodium deoxycholate, 0.1% SDS, 100 µg/mL phenyl-methylsulfonyl fluoride, 10 µg/mL aprotinin, 10 µg/mL leupeptin), incubating the cell solution for 30 min with occasional rocking, and clarifying the solution by centrifugation at 12 000 × g at 4°C for 15 min. The supernatant containing total cell lysate was stored at -80°C until it was ready for use. The protein concentration was determined by the Bradford method. Western blot analysis was performed as previously described^[24]. Briefly, proteins were separated by 10% sodium dodecyl sulfate polyacrylamide gel electrophoresis (SDS-PAGE) and transferred to polyvinylidene difluoride membranes. After being blocked in 5% skim milk at room temperature for 2 h, membranes were subsequently probed with primary antibodies at 4°C overnight. Then the membranes were washed three times with TBST buffer [10 mmol/L Tris-HCl (pH 8.0), 150 mmol/L NaCl, and 0.1% Tween 20] and incubated with secondary antibody at room temperature for 2 h.

Proteins were detected using the enhanced chemiluminescence detection system (Amersham).

Fluorescence microscopy

S1-M1-80 and xS1-M1-80 cells were seeded at a density of 5 × 10⁵ cells/well in 6-well plates and incubated for 24 h to allow cell attachment. The chambers were washed twice with PBS, and fixed with 4% formaldehyde for 15 min at room temperature. Then, cells were washed three times with wash buffer (Immunol Fluorescence Staining Kit, Beyotime). Nonspecific binding sites were blocked for 60 min at room temperature with confining liquid. Then, without further washing, cells were incubated with a rabbit anti-ABCG2 monoclonal antibody BXP-21, diluted at 1:50 with confining liquid, for 60 min at room temperature. ABCG2 staining was revealed by incubation with FITC-conjugated goat anti-rabbit antibody (1:500) for 60 min at room temperature. Cell nuclei were stained with propidium iodide (5 µg/mL) for 5 min at room temperature. Then, the cells were observed under an inverted fluorescence microscope with standard excitation filters in random microscopic fields at ×400 magnification.

Accumulations of doxorubicin and rhodamine 123

To evaluate ABCG2-mediated efflux, the intracellular accumulation of doxorubicin and rhodamine 123 were examined by flow cytometry^[25]. S1-M1-80 and xS1-M1-80 cells were seeded at a density of 5 × 10⁵ cells/well in 6-well plates and incubated at 37°C overnight. Cells were then treated with or without Ko143 (1 µmol/L) at 37°C for 3 h. Then, doxorubicin (10 µmol/L) or rhodamine 123 (5 µg/mL) was added and cells were incubated for another 3 h or 0.5 h, respectively. Finally, the cells were washed with ice-cold PBS three times and resuspended in 500 µL PBS for flow cytometry (FCM, Beckman Coulter, Cytomics FC500, USA). A minimum of 10 000 cells were analyzed for each histogram generated.

Detection of cell surface expression of ABCG2 by flow cytometry

S1-M1-80 and xS1-M1-80 cells were harvested and washed three times with isotonic PBS [supplemented with 0.5% bovine serum albumin (BSA)]. Then, Fc-blocked cells (1 × 10⁶) were incubated with APC-conjugated anti-human BCRP1/ABCG2 antibody (R&D Systems, McKinley Place NE, Minneapolis, USA) for 45 min at 4°C. Finally, the cells were washed twice with PBS (supplemented with 0.5% BSA) and resuspended in 400 µL PBS for FCM. Isotype control samples were treated similarly with an APC-labeled mouse IgG2B

antibody.

Statistical analysis

All data were derived from at least three independent experiments. The difference between two paired groups was evaluated using the Student's *t*-test, which was performed using SPSS 13.0 software (SPSS Inc., Chicago, IL, USA). Differences were considered significant when $P < 0.05$.

Results

S1-M1-80 tumor formation and successful *in vitro* proliferation of xS1-M1-80 cells

Solid tumors were measurable 14 days after inoculation. The overall tumor formation rate was 80% (16/20). The tumor growth curve was drawn according to tumor volume and the time after inoculation (Figure 1). At 63 days after inoculation, when the mean tumor weight was over 1 g, mice were killed. xS1-M1-80 cells were isolated from S1-M1-80 tumor xenografts as described in the Materials and Methods section. Single-cell suspensions from tumors were collected and cultured in DMEM medium.

In vitro growth characteristics of S1-M1-80 and xS1-M1-80 cells

Growth properties of S1-M1-80 cells versus xS1-M1-80 cells growing in monolayer cultures were compared. The *in vitro* proliferating ability of S1-M1-80 and xS1-M1-80 cells were similar (Figure 2A). FCM with propidium iodide staining showed no statistical difference between the two cell lines in terms of cell numbers in the G_0 - G_1 (66.5 ± 10.2 for S1-M1-80 vs. 63.7 ± 11.5 for xS1-M1-80), S (27.8 ± 6.4 vs. 26.2 ± 8.1), and G_2 -M

phases (5.7 ± 2.2 vs. 10.1 ± 2.5) ($P > 0.05$) (Figure 2B).

ABCG2 protein expression in S1-M1-80 cells and xS1-M1-80 cells

ABCG2 protein was highly expressed in S1-M1-80 and xS1-M1-80 cells as determined by Western blotting (Figure 3A). Neither S1-M1-80 cells nor xS1-M1-80 cells showed expression of P-gp and MRP-1; P-gp expression was only detected in positive control KBv200 cells, and MRP-1 expression was only detected in positive control CA120 cells. ABCG2 expression was not detected in S1 cells, and similar surface expression of ABCG2 was confirmed by FCM (Figure 3B).

To investigate the subcellular localization of ABCG2 in S1-M1-80 and xS1-M1-80 cells, cells were stained with the ABCG2 monoclonal antibody BXP-21 followed by a FITC-conjugated secondary antibody. Immunofluorescence scanning microscopy showed positive staining of ABCG2 in the intracellular compartment and on the plasma membrane of the two cell lines (Figure 3C).

Cell sensitivity to chemotherapeutic agents

The drug sensitivities of S1-M1-80 and xS1-M1-80 cells determined by MTT assays are shown in Table 1. S1-M1-80 cells were 90-fold more resistant to mitoxantrone than sensitive S1 cells and displayed 150-fold resistance to topotecan. xS1-M1-80 cells were 91- and 147-fold resistant to mitoxantrone and topotecan, respectively. Ko143 ($1 \mu\text{mol/L}$) effectively reversed mitoxantrone and topotecan resistance and sensitized the resistant S1-M1-80 cells by 87- and 90-fold, respectively, to these agents. Similar results were also obtained with xS1-M1-80 cells: Ko143 sensitized the resistant cells by 94- and 96-fold to mitoxantrone and topotecan, respectively. Both cell lines displayed similar sensitivity to cisplatin, which is not an

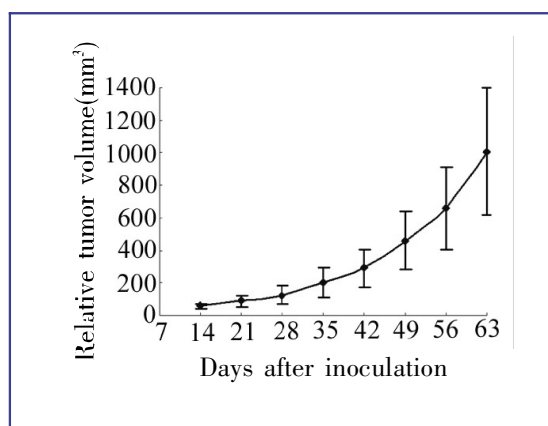


Figure 1. Establishment of S1-M1-80 tumor xenografts. A total of 20 mice were inoculated with S1-M1-80 cells in the right flank. Solid tumors formed in 16 (80%) mice. At 63 days after inoculation, the mean tumor weight was over 1 g. Each point represents the mean \pm standard deviation (SD) of tumor volumes in the 16 mice.

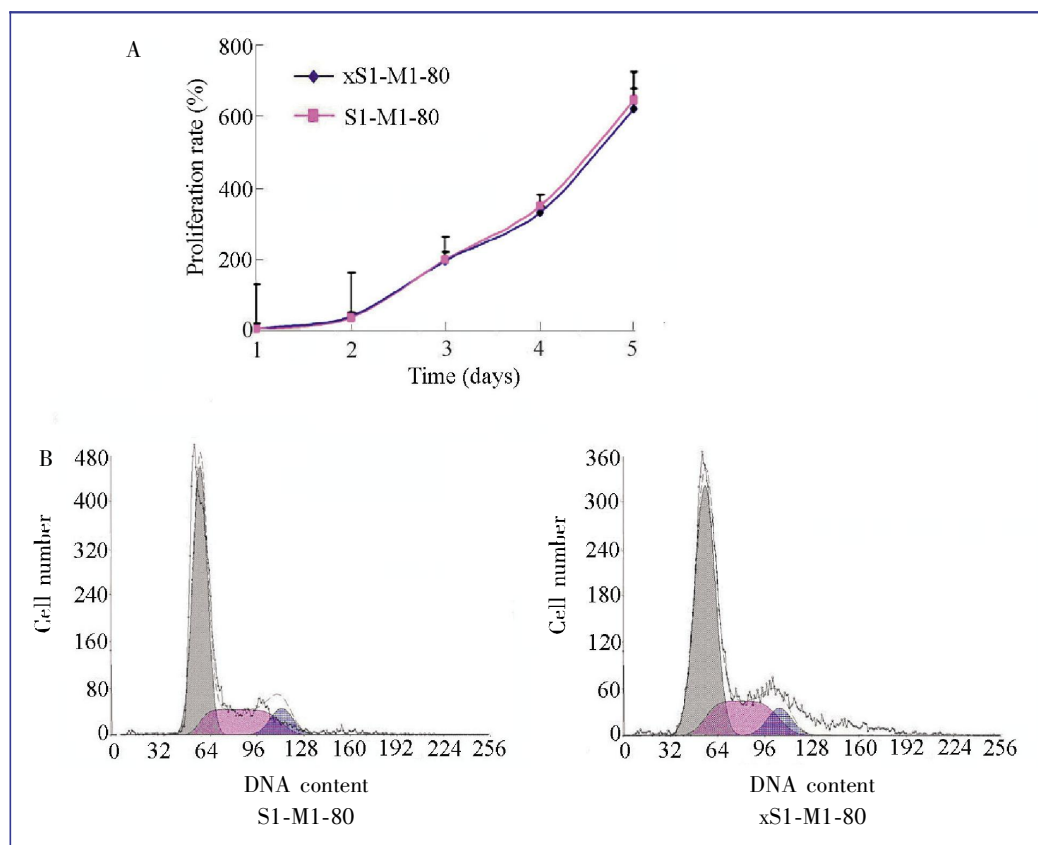


Figure 2. Proliferation and cell cycle of S1-M1-80 and xS1-M1-80 cells. A, the proliferation curves of S1-M1-80 and xS1-M1-80 cells. B, the percentages of the cell population at the G₀-G₁, S, and G₂-M phases were calculated from histograms using the CellQuest software. Data points represent the mean \pm SD of three independent experiments. Cell cycle analysis was performed on a flow cytometer.

ABCG2 substrate, and Ko143 had no reversal effect to cisplatin and on the sensitivity of parental S1 cells.

Accumulation of doxorubicin and rhodamine 123

The intracellular accumulation of doxorubicin and rhodamine 123 were 1.0- and 1.1-fold higher, respectively, in xS1-M1-80 cells than in S1-M1-80 cells. In the presence of Ko143 (1 μ mol/L), the level of doxorubicin accumulation was increased by 6.2- and 6.3-fold for S1-M1-80 and xS1-M1-80 cells, respectively. The intracellular rhodamine 123 accumulation was enhanced by 12.1- and 10.1-fold by Ko143 for the two cell lines, respectively. These results indicate a similar ABCG2 transport activity of the two cell lines (Figure 4).

Discussion

Many *in vivo* tumor models have been developed to better understand the precise mechanisms responsible for drug resistance [21,26]. These animal models allow a direct comparison of *in vitro* and *in vivo* resistance. As a drug resistance model with overexpression of ABCG2,

the S1-M1-80 cell line has been widely used in the study of MDR, whereas the S1-M1-80 cell xenografts have been used less frequently. Based on our success with other tumor xenografts in previous studies [21,27], there is no doubt that the S1-M1-80 cell xenografts can serve as useful tools with which to study the effects of ABCG2 overexpression. The similarities between xS1-M1-80 cells and *in vitro* cultured S1-M1-80 cells deserve further investigation to determine whether the xenograft models reproduce the biological evolution of S1-M1-80 cells. In our study, we demonstrated that the S1-M1-80 cell xenografts in nude mice retain their MDR phenotype and original cytological characteristics, which suggests that the S1-M1-80 cell xenograft model may be useful in preclinical studies of drug resistance *in vivo*.

The MDR phenotype is associated with decreased intracellular drug accumulation resulting from energy-dependent drug efflux. Mitoxantrone resistance appears to be a universal characteristic of cell lines that overexpress ABCG2. To determine whether drug resistance occurs in xS1-M1-80 cells, S1-M1-80 and xS1-M1-80 cells were assayed for sensitivity to mitoxantrone and topotecan. Our data clearly showed that the cross-resistance patterns are almost identical for S1-M1-80 and xS1-M1-80 cells, both having a high level

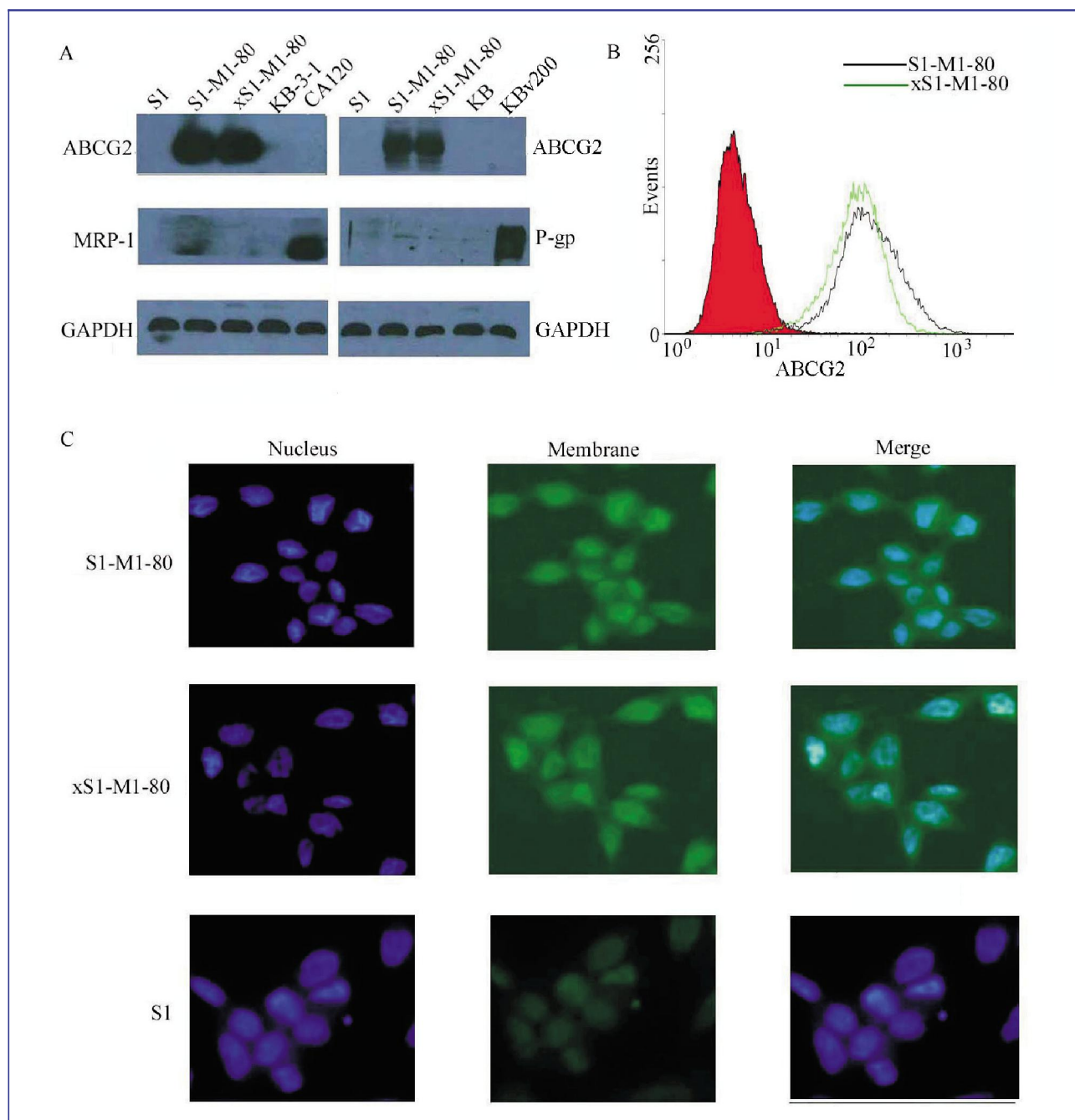


Figure 3. Expression of ABCG2 in S1-M1-80 and xS1-M1-80 cells. A, equal amounts of protein from various cell lines were loaded for Western blotting as described in the Materials and Methods section. S1-M1-80 and xS1-M1-80 cells show high expression of ABCG2 protein but no expression of P-gp or MRP-1. B, flow cytometry was performed as described in the Materials and Methods section. Similar surface expression of ABCG2 is detected in S1-M1-80 and xS1-M1-80 cells. C, immunofluorescence scanning microscopy shows positive staining of ABCG2 in the intracellular compartment and on the plasma membrane of S1-M1-80 and xS1-M1-80 cells.

of resistance to mitoxantrone and topotecan and showing no cross-resistance to cisplatin.

Position 482 is critical for substrate recognition by ABCG2, and mutations at this position significantly

impact substrate specificity^[17,28]. Rhodamine 123 is a substrate for ABCG2_{Gly}, but not for ABCG2_{Arg}. xS1-M1-80 cells exhibited a decrease in rhodamine 123 accumulation similar to the ABCG2_{Gly}-expressing

Table 1. Cytotoxicity of mitoxantrone, topotecan, and cisplatin and the reversal effects of Ko143 in colon carcinoma cells

Compounds	IC ₅₀ [μmol/L (fold-reversal)]		
	S1	S1-M1-80	xS1-M1-80
Mitoxantrone	0.33 ± 0.01	30.03 ± 3.28	30.20 ± 4.62
Mitoxantrone + Ko143	0.31 ± 0.03 (0.94)	0.34 ± 0.10 (88.32)	0.32 ± 0.08 (94.38)
Topotecan	0.28 ± 0.05	42.16 ± 4.54	41.10 ± 4.65
Topotecan + Ko143	0.28 ± 0.04 (1.00)	0.47 ± 0.10 (89.70)	0.43 ± 0.06 (95.58)
Cisplatin	1.81 ± 0.38	1.94 ± 0.39	1.77 ± 0.52
Cisplatin + Ko143	1.57 ± 0.35 (0.87)	1.64 ± 0.43 (0.85)	1.48 ± 0.38 (0.84)

Cell survival was determined by MTT assay as described in the Materials and Methods section. IC₅₀, 50% inhibition concentration. Data are given as the mean ± standard deviation (SD) of at least three independent experiments. The fold reversal of drug resistance (given in parentheses) was calculated by dividing the IC₅₀ for cells with the anticancer drug in the absence of Ko143 by that obtained in the presence of Ko143.

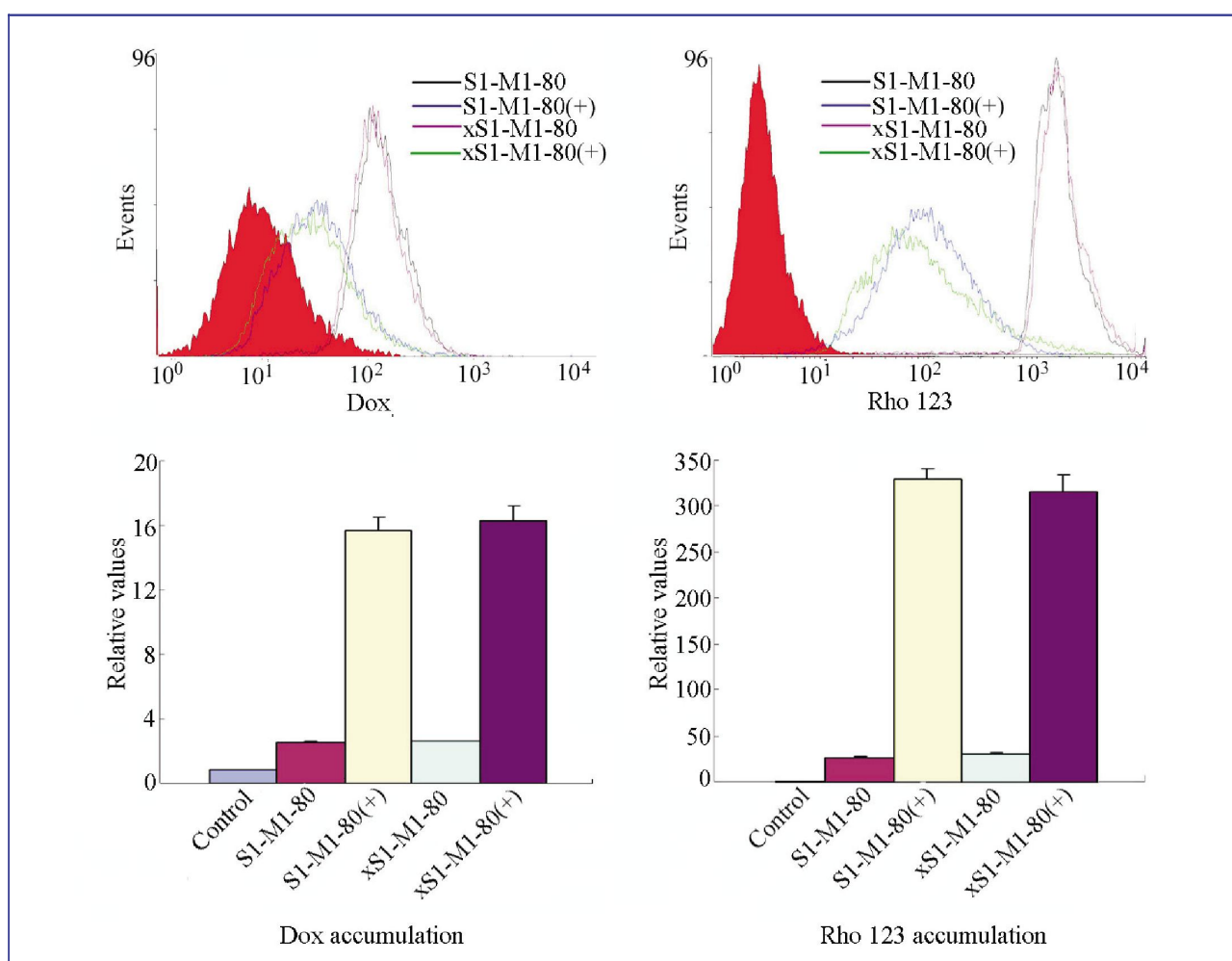


Figure 4. The accumulation of doxorubicin and rhodamine 123 in S1-M1-80 and xS1-M1-80 cells. The accumulation of doxorubicin and rhodamine 123 was measured by flow cytometry as described in the Materials and Methods section. S1-M1-80 and xS1-M1-80 cells treated with 1 μmol/L Ko143 [S1-M1-80(+) and xS1-M1-80(+)] were used as positive controls. The intracellular accumulation in S1-M1-80 and xS1-M1-80 cells were almost identical and were significantly increased in the presence of Ko143. Data points represent the mean ± SD of triplicate experiments.

S1-M1-80 cells, further demonstrating that xS1-M1-80 cells well reproduced the tumor cell cytological characteristics. Furthermore, equal ABCG2 overexpression level was detected in the two cell lines and no detectable expression of P-gp and MRP1 were found, thereby distinguishing the ABCG2 resistance mechanism from that of both P-gp and MRP1.

Our results showed that xS1-M1-80 cells shared similar features with S1-M1-80 cells in several ways. First, we did not observe differences in the ABCG2 protein expression between S1-M1-80 and xS1-M1-80 cells, nor did we detect the expression of other MDR transporters in either cell line. Second, ABCG2 conferred a similar level of resistance to mitoxantrone and other ABCG2 substrates, and the drug resistance was effectively reversed by Ko143. Moreover, S1-M1-80 and xS1-M1-80 cells were equally sensitive to the non-ABCG2 substrate cisplatin. Finally, similar ABCG2 function was detected based on fluorescent doxorubicin

and rhodamine 123 accumulation and the ability of Ko143 to significantly raise the accumulation of these agents in the two cell lines.

In summary, we have developed a xenograft model of S1-M1-80 cells in nude mice that reproduces the biological evolution of S1-M1-80 cells. The similarities between xS1-M1-80 cells and *in vitro* cultured S1-M1-80 cells support the assumption that the tumor cells retain their original cytological characteristics after the xenografts are established in mice. Thus, heterotransplantation of human colon carcinoma in nude mice can serve as a useful technique with which to study ABCG2-mediated drug resistance *in vivo*. It may also serve as a pharmacologic model for screening new potential anticancer agents.

Received: 2011-07-28; revised: 2012-01-10;
accepted: 2012-01-12.

References

- [1] Gottesman MM, Ambudkar SV. Overview: ABC transporters and human disease. *J Bioenerg Biomembr*, 2001,33:453–458.
- [2] Sarkadi B, Homolya L, Szakacs G, et al. Human multidrug resistance ABCB and ABCG transporters: participation in a chemoinnate defense system. *Physiol Rev*, 2006,86:1179–1236.
- [3] Szakacs G, Paterson JK, Ludwig JA, et al. Targeting multidrug resistance in cancer. *Nat Rev Drug Discov*, 2006,5:219–234.
- [4] Allen JD, Schinkel AH. Multidrug resistance and pharmacological protection mediated by the breast cancer resistance protein (BCRP/ABCG2). *Mol Cancer Ther*, 2002,1:427–434.
- [5] Maliepaard M, Scheffer GL, Faneyte IF, et al. Subcellular localization and distribution of the breast cancer resistance protein transporter in normal human tissues. *Cancer Res*, 2001,61:3458–3464.
- [6] Shimano K, Satake M, Okaya A, et al. Hepatic oval cells have the side population phenotype defined by expression of ATP-binding cassette transporter ABCG2/BCRP1. *Am J Pathol*, 2003,163:3–9.
- [7] Krishnamurthy P, Ross DD, Nakanishi T, et al. The stem cell marker Bcrp/ABCG2 enhances hypoxic cell survival through interactions with heme. *J Biol Chem*, 2004,279:24218–24225.
- [8] Maliepaard M, van Gastelen MA, de Jong LA, et al. Overexpression of the BCRP/MXR/ABCP gene in a topotecan-selected ovarian tumor cell line. *Cancer Res*, 1999,59:4559–4563.
- [9] Brangi M, Litman T, Ciotti M, et al. Camptothecin resistance: role of the ATP-binding cassette (ABC), mitoxantrone-resistance half-transporter (MXR), and potential for glucuronidation in MXR-expressing cells. *Cancer Res*, 1999,59:5938–5946.
- [10] Kawabata S, Oka M, Shiozawa K, et al. Breast cancer resistance protein directly confers SN-38 resistance of lung cancer cells. *Biochem Biophys Res Commun*, 2001,280:1216–1223.
- [11] Tsunoda S, Okumura T, Ito T, et al. ABCG2 expression is an independent unfavorable prognostic factor in esophageal squamous cell carcinoma. *Oncology*, 2006,71:251–258.
- [12] Svirnovski AI, Shman TV, Serhiyenko TF, et al. ABCB1 and ABCG2 proteins, their functional activity and gene expression in concert with drug sensitivity of leukemia cells. *Hematology*, 2009,14:204–212.
- [13] Damiani D, Tiribelli M, Michelutti A, et al. Fludarabine-based induction therapy does not overcome the negative effect of ABCG2 (BCRP) over-expression in adult acute myeloid leukemia patients. *Leuk Res*, 2010,34:942–945.
- [14] Nakanishi T, Ross DD. Breast cancer resistance protein (BCRP/ABCG2): its role in multidrug resistance and regulation of its gene expression. *Chin J Cancer*, 2012,31:73–99.
- [15] Kim YH, Ishii G, Goto K, et al. Expression of breast cancer resistance protein is associated with a poor clinical outcome in patients with small-cell lung cancer. *Lung Cancer*, 2009,65:105–111.
- [16] Jonker JW, Buitelaar M, Wagenaar E, et al. The breast cancer resistance protein protects against a major chlorophyll-derived dietary phototoxin and protoporphyria. *Proc Natl Acad Sci U S A*, 2002,99:15649–15654.
- [17] Honjo Y, Hrycyna CA, Yan QW, et al. Acquired mutations in the MXR/BCRP/ABCP gene alter substrate specificity in MXR/BCRP/ABCP-overexpressing cells. *Cancer Res*, 2001,61:6635–6639.
- [18] Dai CL, Xiong HY, Tang LF, et al. Tetrandrine achieved plasma concentrations capable of reversing MDR *in vitro* and had no apparent effect on doxorubicin pharmacokinetics in mice. *Cancer Chemother Pharmacol*, 2007,60:741–750.
- [19] Sumizawa T, Chuman Y, Sakamoto H, et al. Non-P-glycoprotein-mediated multidrug-resistant human KB cells selected in medium containing adriamycin, cepharanthine, and mezerein. *Somat Cell Mol Genet*, 1994,20:423–435.
- [20] Litman T, Brangi M, Hudson E, et al. The multidrug-resistant phenotype associated with overexpression of the new ABC half-transporter, MXR (ABCG2). *J Cell Sci*, 2000,113:2011–2021.
- [21] Dai CL, Tiwari AK, Wu CP, et al. Lapatinib (Tykerb, GW572016) reverses multidrug resistance in cancer cells by

- inhibiting the activity of ATP-binding cassette subfamily B member 1 and G member 2. *Cancer Res*, 2008,68:7905–7914.
- [22] Shi Z, Liang YJ, Chen ZS, et al. Reversal of MDR1/P-glycoprotein-mediated multidrug resistance by vector-based RNA interference *in vitro* and *in vivo*. *Cancer Biol Ther*, 2006,5: 39–47.
- [23] Cai MJ, Xie RF, Han L, et al. Effect of RNAi-mediated LRIG3 gene silencing on proliferation of glioma GL15 cells and expression of PCNA and Ki-67. *Ai Zheng*, 2009,28:1–4.
- [24] Zhang JY, Wu HY, Xia XK, et al. Anthracenedione derivative 1403P-3 induces apoptosis in KB and KBv200 cells via reactive oxygen species-independent mitochondrial pathway and death receptor pathway. *Cancer Biol Ther*, 2007,6:1413–1421.
- [25] Fu L, Liang Y, Deng L, et al. Characterization of tetrandrine, a potent inhibitor of P-glycoprotein-mediated multidrug resistance. *Cancer Chemother Pharmacol*, 2004,53:349–356.
- [26] Schechter RL, Woo A, Duong M, et al. *In vivo* and *in vitro* mechanisms of drug resistance in a rat mammary carcinoma model. *Cancer Res*, 1991,51:1434–1442.
- [27] Mi YJ, Liang YJ, Huang HB, et al. Apatinib (YN968D1) reverses multidrug resistance by inhibiting the efflux function of multiple ATP-binding cassette transporters. *Cancer Res*, 2010,70:7981–7991.
- [28] Allen JD, Jackson SC, Schinkel AH. A mutation hot spot in the Bcrp1 (Abcg2) multidrug transporter in mouse cell lines selected for Doxorubicin resistance. *Cancer Res*, 2002,62: 2294–2299.

Submit your next manuscript to *Chinese Journal of Cancer* and take full advantage of:

- Open access
- No charge to authors
- Quickly published
- Thorough peer review
- Professionally edited
- No space constraints
- Indexed by PubMed, CA, and Google Scholar

Submit your manuscript at
www.cjcsysu.com